Available online at www.sciencedirect.com
SCIENCE DIRECT
Journal of Organometallic Chemistry 691 (2006) 2933–2944
Journal of Organometallic Chemistry
www.elsevier.com/locate/jorganchem

Switching of global minima of novel germylenic reactive intermediates via halogens (X): C_2GeH_2 vs. C_2GeHX at ab initio and DFT levels

M.Z. Kassaee *, S.M. Musavi, M. Ghambarian, M.R. Khalili Zanjani

Department of Chemistry, Tarbiat Modarres University, P.O. Box 14155-4838, Tehran, Iran

Received 25 December 2005; received in revised form 24 February 2006; accepted 28 February 2006
Available online 6 March 2006

Abstract

For 30 C_2GeHX germylenic isomers, one cyclic structure, X-germacyclopropenylidene, and three acyclics are considered, which include: ethynyl-X-germylene, X-vinylidenegermylene, and (X-ethynyl)germylene (X = H, F, Cl, and Br). The global minimum among six isomeric C_2GeH_2 (where X = H), is found to be cyclic, aromatic, singlet germacyclopropenylidene. In contrast, among the 24 corresponding halogermylenes, C_2GeHX (where X = F, Cl, and Br), the global minima switch to acyclic, singlet ethynylhalogermylenes, at eight reasonably high ab initio and DFT levels. The direct resonance interaction between X and the divalent center Ge in the singlet acyclic ethynylhalogermylene structures, is claimed to justify switching of the calculated global minima in the halo derivatives. GIAO–NICS calculations indicate that the X-germacyclopropenylidene isomer is more aromatic for X = H than X = F, Cl, or Br. The angle ∠XGeC bending potential energy curves show the singlet and triplet ethynylgermylene crossing at ≈146°, for X = H.

Keywords: Germylene; LUMO–HOMO; C_2GeH_2; C_2GeHF; C_2GeHCl; C_2GeHBr; Halogermacyclopropenylidene; Ethynylhalogermylene; Haloethynylgermylene; Vinylidengermylene; Ab initio; DFT; NICS

1. Introduction

During the past two decades, much attention has been devoted to the heavier carbene analogues consisting of silylenes R_2Si [1,2] and germylenes R_2Ge [3]. In these cases the ground state electronic configurations can be either singlet or triplet, depending on many factors. An excellent review describing silylene and germylene electronic structure and reactivity has been published by Nefedov et al. [4], wherein the main features of these carbene-like molecules on going from carbon to lead are discussed in detail from the available experimental data. There have been a large number of theoretical studies to examine the low-lying electronic states of methylene [5], halogenated carbenes [6] and unsaturated carbenes [7]. The major aim of these works is to ascertain the nature of the ground state, to calculate the singlet–triplet ($^1A_1$–$^3B_1$) energy separations (ΔE_{s-t}), and to compare the theoretical and experimental results. Similar studies are also reported on the simplest silylene (SiH_2) [8–10] and silicondifluoride (SiF_2) [11,12].

The initial theoretical investigations on R_2Ge have shown a strong propensity for germylenes to have singlet ground states, where the ΔE_{s-t} are much higher than those of carbenes, but are not very much higher than the silylenes [13]. Moreover, the higher ΔE_{s-t} of GeF_2 compared to $GeMe_2$ and/or GeH_2 is consistent with the stronger electrophilic activity of GeF_2. With respect to ground-state multiplicity of group 14 divalent compounds, the main change seems to occur from second row (C) to third row (Si) elements [14]. Changing the group IV atom does not seem to lead to major structural differences in silylenes and germylenes. A subtle and interesting difference occurs, for

* Corresponding author. Tel.: +011 98 912 100392; fax: +98 21 8006544.
E-mail address: Kassaeem@Modares.ac.ir (M.Z. Kassaee).

0022-328X/$ - see front matter © 2006 Elsevier B.V. All rights reserved.
doi:10.1016/j.jorganchem.2006.02.038

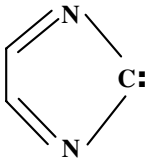

Scheme 1. A general structure for imidazol-2-ylidene derivatives.

instance, in the structure of the difluoride dimer which is bridged for GeF_2 [15] and π-bonded for SiF_2 [16].

Unsaturated carbenes, silylenes and germylenes, with imidazol-2-ylidene structures (Scheme 1), have been synthesized and theoretically investigated [17–20]. The enhanced p_π–p_π delocalization of these structures, leads to a significant electronic charge in the formally "empty" p_π orbital of the divalent atom and strong stabilization by electron donation from the nitrogen lone pairs into the formally "empty" p_π orbital.

To gain more comprehensive insights into the electronic structures and energetics of divalent group 14 species we recently studied the derivatives of C_3H_2 carbenes [21–24] and C_2H_2Si silylenes [25,26]. Following on our previous studies, the primary goal of the present work is the use of reasonable high-level theoretical procedures to determine the singlet–triplet splittings and relative stabilities in the isomeric forms of halo-substituted C_2GeHX germylenes, for X = H, F, Cl, and Br (**1**–**4**, Fig. 1).

2. Computational methods

All calculations are performed using the GAUSSIAN 98 program package [27]. The geometries and energies of singlet and triplet germylenes are fully optimized without imposing any symmetry constraints. For Hartree-Fock (HF) level, 6-311++G** basis set is used. For DFT calculations the Becke's hybrid one-parameter and three-parameter functional using the non-local LYP correlation [28,29] with the 6-311++G** and 6-311++G** basis sets are employed. For B3LYP method the LANL2DZ basis set is also employed [30]. For the second-order MØller–Plesset (MP2) method the 6-311++G** basis sets is used [31]. The MP2/6-311++G** optimized geometries are submitted as inputs for single-point calculations at the MP4, QCISD (T) [32–34] and CCSD (T) levels [35] with 6-311++G** basis set. Singlet states are calculated with spin-restricted wave functions, while the spin projected wave functions are employed for triplet states. Harmonic vibrational frequencies were computed at the HF, B1LYP and B3LYP levels. This was done to characterize the isomers as minima (no imaginary frequencies), transition state (one imaginary frequency), or saddle point of second order (two imaginary frequencies). The vibrational frequencies and ZPE data at the HF and DFT are scaled by 0.89 and 0.98, respectively [36,37]. The NBO population analysis are accomplished at the B3LYP/6-311++G** level [38]. Nucleus independent chemical shifts, NICS values [39], are calculated by the gauge-independent atomic orbital (GIAO) method [40,41] at the B3LYP/6-311++G**. NICS values are measured at the ring center (defined as simple average of Cartesian coordinates for all atoms of three membered ring) as well as 0.5, 1, 1.5, 2, 2.5, and 3 Å above the plane of ring. Gaussian input format requires Cartesian coordinates in order to compute NICS values at various points at and above the center of rings. To input the mass weighted geometrical center is a possibility which is not explored in this manuscript. The keyword "Scan" in Gaussian is used for scanning the bending potential energy curves of ∠CGeX angles, from 60° to 180° with 10° increments, for $\mathbf{2}_{\mathbf{s\text{-}X}}$ and $\mathbf{2}_{\mathbf{t\text{-}X}}$ at B3LYP/6-311++G**.

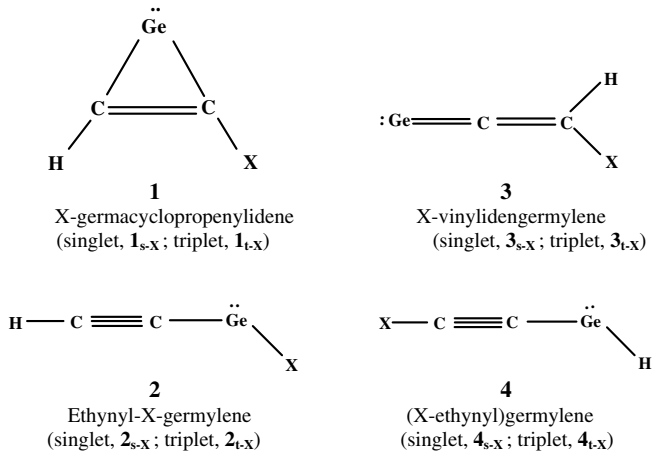

Fig. 1. Singlet (**s**) and triplet (**t**) states for possible germylenic structures of GeC_2HX (**1**, **2**, **3** and **4**, where X = H, F, Cl, and Br).

2.1. General results

Force constant calculations suggest that among 30 germylenic isomers considered here, only triplet $\mathbf{1}_{\mathbf{t\text{-}F}}$ exists as a transition state on the potential energy surface of C_2GeHX, for showing one negative force constant. Computed harmonic frequencies are not provided for the sake of brevity, but are available upon request. Moreover, the cyclic triplet structures $\mathbf{1}_{\mathbf{t\text{-}F}}$ (at B3LYP/6-311++G**), $\mathbf{1}_{\mathbf{t\text{-}H}}$ (at MP2/6-311+G**), and $\mathbf{1}_{\mathbf{t\text{-}Br}}$ (at B3LYP/6-311++G**) collapse to other structures on optimizations. The results of the HF/6-311++G**, B3LYP/LANL2DZ, B1LYP/6-311++G**, B3LYP/6-311++G**, MP2/6-311++G**, MP4(SDTQ)/6-311++G**, QCISD(T)/6-311+G**, and CCSD(T)/6-311++G** energy calculations of all possible structures of halogermylenes, (C_2GeHX, **1**–**4**, X = H, F, Cl, and Br) are shown in Fig. 1 and Tables 1–4. We have deliberately included data from eight levels of theory, since reporting results of various levels may offer an opportunity for comparison of different levels. B3LYP/6-311++G** calculated dipole moments and vibrational zero point energies (ZPE) for C_2GeHX species are also presented (Tables 1–4). Energy results are dependent on the computational

Table 1
Relative energies (kcal/mol), with ZPE corrections, for singlet $\mathbf{1}_{s\text{-}H}$, $\mathbf{2}_{s\text{-}H}$, and $\mathbf{3}_{s\text{-}H}$ as well as triplet states $\mathbf{1}_{t\text{-}H}$, $\mathbf{2}_{t\text{-}H}$, and $\mathbf{3}_{t\text{-}H}$ of germylenic C_2GeH_2, calculated at eight levels of theory; along with dipole moments (Debye) and vibrational zero point energies (kcal/mol) calculated at B3LYP/6-311++G**

Structure	Relative energies (kcal/mol)								Dipole moments (D)	Vibrational zero point energies (kcal/mol)
	HF/ 6-311++G**	B3LYP/ LANL2DZ[a]	B1LYP/ 6-311++G**	B3LYP/ 6-311++G**	[a]MP2/ 6-311++G**	[a]MP4(SDTQ)/ 6-311++G**	[a]QCISD(T)/ 6-311++G**	[a]CCSD(T)/ 6-311++G**	B3LYP/6-311++G**	B3LYP/6-311++G**
$\mathbf{1}_{s\text{-}H}$[b]	0.00[1]	0.00[2]	0.00[3]	0.00[4]	0.00[5]	0.00[6]	0.00[7]	0.00[8]	0.50	17.96
$\mathbf{1}_{t\text{-}H}$	22.47	41.95	40.50	40.97	41.78	41.29	40.77	40.80	1.91	16.45
$\mathbf{2}_{s\text{-}H}$	10.15	15.62	13.64	14.07	18.71	17.18	16.86	16.94	0.39	14.93
$\mathbf{2}_{t\text{-}H}$	23.57	43.38	45.18	45.94	48.83	49.21	46.58	46.73	0.16	14.96
$\mathbf{3}_{s\text{-}H}$	15.03	6.52	11.25	11.21	16.23	12.65	11.82	11.91	0.58	17.54
$\mathbf{3}_{t\text{-}H}$	53.69	25.25	28.54	29.25	42.14	38.13	34.88	35.02	0.98	16.76

The original total energies (hartrees) corresponding to the lowest energy minimum $\mathbf{1}_{s\text{-}H}$ at various levels of theory: (1) −2152.16191, (2) −81.0847999, (3) −2154.298299, (4) −2154.369961, (5) −2152.513367, (6) −2152.555555, (7) −2152.555472, (8) −2152.555091.

[a] ZPE not included.

[b] The lowest energy minimum is set at 0.00 kcal/mol.

Table 2
Relative energies (kcal/mol), with ZPE corrections, for singlet $\mathbf{1}_{s\text{-}F}$, $\mathbf{2}_{s\text{-}F}$, $\mathbf{3}_{s\text{-}F}$, and $\mathbf{4}_{s\text{-}F}$ as well as triplet states $\mathbf{2}_{t\text{-}F}$, $\mathbf{3}_{t\text{-}F}$, and $\mathbf{4}_{t\text{-}F}$ ($\mathbf{1}_{t\text{-}F}$ is not an isomer) of germylenic C_2GeHF, calculated at eight levels of theory; along with dipole moments (Debye) and vibrational zero point energies (kcal/mol) calculated at B3LYP/6-311++G**

Structure	Relative energies (kcal/mol)								Dipole moments (D)	Vibrational zero point energies (kcal/mol)
	HF/ 6-311++G**	B3LYP/ LANL2DZ[a]	B1LYP/ 6-311++G**	B3LYP/ 6-311++G**	MP2/ 6-311++G**[a]	MP4(SDTQ)/ 6-311++G**[a]	QCISD(T)/ 6-311++G**[a]	CCSD(T)/ 6-311++G**[a]	B3LYP/6-311++G**	B3LYP/6-311++G**
$\mathbf{1}_{s\text{-}F}$	29.70	31.42	26.54	25.89	25.80	25.05	24.40	24.24	1.63	13.56
$\mathbf{2}_{s\text{-}F}$[b]	0.00[1]	0.00[2]	0.00[3]	0.00[4]	0.00[5]	0.00[6]	0.00[7]	0.00[8]	2.69	12.36
$\mathbf{2}_{t\text{-}F}$	37.05	52.40	56.39	56.67	53.49	56.15	53.87	53.90	2.60	12.25
$\mathbf{3}_{s\text{-}F}$	41.71	35.20	34.78	34.09	36.83	33.64	32.57	32.56	1.74	13.68
$\mathbf{3}_{t\text{-}F}$	49.37	64.96	63.35	63.82	74.49	146.16	140.26	139.49	1.49	12.98
$\mathbf{4}_{s\text{-}F}$	53.23	63.36	53.47	54.10	92.43	92.12	90.42	90.15	0.36	10.76
$\mathbf{4}_{t\text{-}F}$	68.34	92.18	86.05	87.11	122.13	124.05	120.65	120.40	0.38	10.74

The original total energies (hartrees) corresponding to the lowest energy minimum $\mathbf{2}_{s\text{-}F}$ at various levels of theory: (1) −2251.084898, (2) −180.3791853, (3) −42253.589743, (4) −2253.677782, (5) −2251.630866, (6) −2251.675705, (7) −2251.671919, (8) −2251.670671.

[a] ZPE not included.

[b] The lowest energy minimum is set at 0.00 kcal/mol.

Table 3
Relative energies (kcal/mol), with ZPE corrections, for singlet $\mathbf{1}_{s\text{-}Cl}$, $\mathbf{2}_{s\text{-}Cl}$, $\mathbf{3}_{s\text{-}Cl}$, and $\mathbf{4}_{s\text{-}Cl}$ as well as triplet states $\mathbf{1}_{t\text{-}Cl}$, $\mathbf{2}_{t\text{-}Cl}$, $\mathbf{3}_{t\text{-}Cl}$, and $\mathbf{4}_{t\text{-}Cl}$ of germylenic C_2GeHCl, calculated at eight levels; along with dipole moments (Debye) and vibrational zero point energies (kcal/mol) calculated at B3LYP/6-311++G**

Structure	Relative energies (kcal/mol)								Dipole moments (D)	Vibrational zero point energies (kcal/mol)
	HF/ 6-311++G**	B3LYP/ LANL2DZ[a]	B1LYP/ 6-311++G**	B3LYP/ 6-311++G**	MP2/ 6-311++G**[a]	MP4(SDTQ)/ 6-311++G**[a]	QCISD(T)/ 6-311++G**[a]	CCSD(T)/ 6-311++G**[a]	B3LYP/6-311++G**	B3LYP/6-311++G**
$\mathbf{1}_{s\text{-}Cl}$	30.17	28.30	25.08	24.40	20.53	20.84	21.56	21.46	1.60	12.72
$\mathbf{1}_{t\text{-}Cl}$	55.86	75.36	74.16	73.84	72.58	72.50	72.85	72.76	1.34	11.36
$\mathbf{2}_{s\text{-}Cl}$[b]	0.00[1]	0.00[2]	0.00[3]	0.00[4]	0.00[5]	0.00[6]	0.00[7]	0.00[8]	2.58	11.97
$\mathbf{2}_{t\text{-}Cl}$	31.20	46.53	49.74	50.06	47.73	49.59	47.36	47.39	1.91	11.91
$\mathbf{3}_{s\text{-}Cl}$	46.03	32.99	36.17	35.36	35.57	32.94	33.10	33.17	1.71	12.71
$\mathbf{3}_{t\text{-}Cl}$	50.18	59.30	60.50	60.77	68.97	65.09	62.01	61.99	1.27	12.07
$\mathbf{4}_{s\text{-}Cl}$	49.30	56.21	47.29	47.33	47.38	46.20	46.83	46.79	0.29	9.86
$\mathbf{4}_{t\text{-}Cl}$	63.39	84.60	79.19	79.46	78.39	79.12	77.30	77.30	0.12	9.73

The original total energies (hartrees) corresponding to the lowest energy minimum $\mathbf{2}_{s\text{-}Cl}$ at various levels of theory: (1) −2611.136631,(2) −95.4734821, (3) −2613.95419, (4) −2614.03685, (5) −2611.609137, (6) −2611.662824, (7) −2611.662688, (8) −2611.661914.

[a] ZPE not included.

[b] The lowest energy minimum is set at 0.00 kcal/mol.

Table 4
Relative energies (kcal/mol), with ZPE corrections, for singlet $\mathbf{1}_{s\text{-}Br}$, $\mathbf{2}_{s\text{-}Br}$, $\mathbf{3}_{s\text{-}Br}$, and $\mathbf{4}_{s\text{-}Br}$ as well as triplet states $\mathbf{1}_{t\text{-}Br}$, $\mathbf{2}_{t\text{-}Br}$, $\mathbf{3}_{t\text{-}Br}$, and $\mathbf{4}_{t\text{-}Br}$ of germylenic C_2GeHBr, calculated at eight levels of theory; along with dipole moments (Debye) and vibrational zero point energies (kcal/mol) calculated at B3LYP/6-311++G**

Structure	Relative energies (kcal/mol)								Dipole moments (D)	Vibrational zero point energies (kcal/mol)
	HF/ 6-311++G**	B3LYP/ LANL2DZ[a]	B1LYP/ 6-311++G**	B3LYP/ 6-311++G**	MP2/ 6-311++G**[b]	MP4(SDTQ)/ 6-311++G**[b]	QCISD(T)/ 6-311++G**[b]	CCSD(T)/ 6-311++G**[b]	B3LYP/6-311++G**	B3LYP/6-311++G**
$\mathbf{1}_{s\text{-}Br}$	31.35	–	25.80	25.13	21.74	22.08	23.01	22.91	1.69	12.40
$\mathbf{1}_{t\text{-}Br}$	56.31	–	59.58	59.59	73.08	72.93	73.37	73.28	1.61	10.98
$\mathbf{2}_{s\text{-}Br}$[c]	0.00[1]	–[2]	0.00[3]	0.00[4]	0.00[5]	0.00[6]	0.00[7]	0.00[8]	2.44	11.79
$\mathbf{2}_{t\text{-}Br}$	29.44	–	47.27	47.59	46.08	47.69	45.38	45.40	1.49	11.69
$\mathbf{3}_{s\text{-}Br}$	47.61	–	36.90	36.06	37.47	34.84	35.15	35.23	1.87	12.32
$\mathbf{3}_{t\text{-}Br}$	51.04	–	60.26	60.48	69.40	77.76	62.60	62.61	1.15	11.67
$\mathbf{4}_{s\text{-}Br}$	50.35	–	39.09	48.14	48.84	47.52	48.31	48.27	0.45	9.48
$\mathbf{4}_{t\text{-}Br}$	64.20	–	70.92	80.21	80.22	80.72	78.81	78.81	0.31	9.43

The original total energies (hartrees) corresponding to the lowest energy minimum $\mathbf{3}_{s\text{-}Br}$ at various levels of theory: (1) −4724.001495, (2) – , (3) −4727.8733, (4) −4727.960662, (5) −4724.460457, (6) −4724.512192, (7) −4724.511922, (8) −4724.511152.

[a] The calculations at B3LYP/LANL2DZ are not converged.

[b] ZPE not included.

[c] The lowest energy minimum is set at 0.00 kcal/mol.

Table 5
The NICS (total) values (ppm) at the ring centers, NICS(0), and 0.5, 1, 1.5, 2, 2.5, and 3 Å above the plane of the rings (NICS(0.5), NICS(1), NICS(1.5), NICS(2), NICS(2.5), and NICS(3), respectively), for singlet (s) states of C_2GeHX ($\mathbf{1_{s\text{-}X}}$, X = H, F, Cl, and Br) germylenes as well as the cyclopropenyl cation, cyclopropenyl anion, cyclopropenyl radical, cyclopropenylidene (singlet), cyclopropenylidene (triplet) and germacyclopropenyl cation (which are used for comparison), calculated at GIAO-B3LYP/6-311++G**//B3LYP/6-311++G** level

Structure	NICS(0)	NICS(0.5)	NICS(1)	NICS(1.5)	NICS(2)	NICS(2.5)	NICS(3)
$\mathbf{1_{s\text{-}H}}$	−14.18	−17.74	−13.16	−7.15	−3.81	−2.23	−1.45
$\mathbf{1_{s\text{-}F}}$	−18.83	−19.50	−12.17	−5.74	−2.71	−1.47	−0.92
$\mathbf{1_{s\text{-}Cl}}$	−16.11	−18.28	−12.26	−6.10	−3.05	−1.74	−1.12
$\mathbf{1_{s\text{-}Br}}$	−15.34	−17.75	−11.99	−5.97	−2.99	−1.71	−1.11
Cyclopropenyl cation	−22.85	−28.50	−14.69	−6.11	−2.89	−1.60	−1.01
Cyclopropenyl anion	4.20	14.99	16.64	9.79	4.95	2.29	0.95
Cyclopropenyl radical	−9.49	−0.51	5.2	3.25	1.49	0.61	0.21
Cyclopropenylidene (singlet)	−16.76	−27.46	−17.07	−7.79	−3.78	−2.09	−1.30
Cyclopropenylidene (triplet)	−36.86	−20.32	−3.07	0.39	0.56	0.35	0.18
Germacyclopropenyl cation	−14.72	−17.04	−10.28	−4.36	−1.93	−1.07	−0.70

methods employed. Moreover, the energy results obtained at HF level are remote, compared to other calculation methods. Nevertheless, consistency is found between the orders of calculated relative energies (Tables 1–4). The magnitude of energies obtained at B3LYP appears to depend on the applied basis sets. Hence, in contrast to B3LYP/LANL2DZ, the B3LYP/6-311++G** appears to be consistent with the higher level ab initio methods: MP4(SDTQ), QCISD(T), and CCSD(T). The relative energies, calculated at QCISD(T) and CCSD(T) levels, are similar to each other, while they appear somewhat different from those of MP4. These differences are more pronounced for triplet state species, due to the possible spin-contamination problem which has been encountered for MP4(SDTQ) calculations [42,43].

In the following discussion the high level CCSD (T) single-point energy results are preferred while, B3LYP appears reliable for computing geometrical parameters [43]. The NICS values are calculated for singlet cyclic germylenes, $\mathbf{1_{s\text{-}X}}$ (Table 5). Accordingly, the calculated optimized geometries of **1**–**4** are reported, at B3LYP/6-311++G** and MP2/6-311++G** levels (Tables 6–9). Geometrical parameters do not appear to be sensitive to the different levels of theory employed. Nearly similar results are obtained for the geometrical parameters optimized through methods other than B3LYP/6-311++G** and MP2/6-311++G** which are not included in Tables 6–9. All optimized structures are planar with at least C_s symmetry. Atomic charges and bond orders are derived from the NBO population analysis at B3LYP/6-311++G** (Table 10) [38]. The NBO method provides an orbital picture which is closer to the classical Lewis structure. The energies of the HOMO and LUMO orbitals are obtained for both singlet and triplet isomers of C_2GeHX. LUMO–HOMO energy gaps of the singlet germylenes $\mathbf{1_{s\text{-}X}}$–$\mathbf{4_{s\text{-}X}}$, show linear correlations between their corresponding singlet–triplet energy separations, calculated at B3LYP/6-311++G** level of theory (Fig. 2). Halogens increase the magnitude of LUMO–HOMO energy gaps. The correlation coefficient trend is: $\mathbf{3_{s\text{-}X}}$ ($R^2 = 0.98$) > $\mathbf{4_{s\text{-}X}}$ ($R^2 = 0.97$) > $\mathbf{2_{s\text{-}X}}$ ($R^2 = 0.94$) > $\mathbf{1_{s\text{-}X}}$ ($R^2 = 0.70$), where R^2 is the correlation coefficient. The highest LUMO–HOMO energy gaps are found for singlet cyclic structures $\mathbf{1_{s\text{-}X}}$. While, due to the distance of X from the divalent center, the lowest range of LUMO–HOMO energy gaps as a function of substituents X, are encountered for $\mathbf{4_{s\text{-}X}}$ species.

Table 6
Optimized geometrical parameters (bond distances (R) and bond angles (A)) along with symmetry, for singlet (**s**) and triplet (**t**) X-germacyclopropenylidene ($\mathbf{1_{s\text{-}x}}$ and $\mathbf{1_{t\text{-}x}}$), at two levels of theory: first line, B3LYP/6-311++G**; second line, *MP2/6-311++G** in italics* (where X = H, F, Cl, and Br)

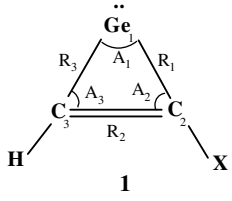

1

Structure/symmetry	Bond distances (Å)			Bond angles (°)		
	R_1	R_2	R_3	A_1	A_2	A_3
$\mathbf{1_{s\text{-}H}}(C_{2v})$	1.94	1.33	1.94	40.2	69.9	69.9
	1.94	*1.35*	*1.94*	*40.5*	*69.7*	*69.7*
$\mathbf{1_{s\text{-}F}}(C_s)$	1.92	1.33	1.96	39.9	71.6	68.4
	1.93	*1.34*	*1.98*	*40.0*	*71.8*	*68.2*
$\mathbf{1_{s\text{-}Cl}}(C_s)$	1.93	1.33	1.95	39.9	71.0	69.0
	1.93	*1.34*	*1.96*	*40.3*	*70.6*	*69.0*
$\mathbf{1_{s\text{-}Br}}(C_s)$	1.94	1.33	1.96	39.8	71.1	69.0
	1.94	*1.34*	*1.96*	*40.3*	*70.7*	*69.0*
$\mathbf{1_{t\text{-}H}}(C_{2v})$[a]	2.36	1.23	2.36	30.2	74.9	74.9
	–	–	–	–	–	–
$\mathbf{1_{t\text{-}F}}(C_s)$[a]	–	–	–	–	–	–
	2.28	*1.25*	*2.35*	*31.3*	*77.1*	*71.4*
$\mathbf{1_{t\ Cl}}(C_s)$[a]	2.39	1.26	2.14	31.6	63.1	85.2
	2.30	*1.25*	*2.33*	*31.3*	*75.9*	*72.8*
$\mathbf{1_{t-Br}}(C_s)$	–	–	–	–	–	–
	2.29	*1.25*	*2.33*	*31.5*	*75.6*	*72.9*

[a] Rupture upon optimization.

Table 7
Optimized geometrical parameters (bond distances (R) and bond angles (A)) along with symmetry, for singlet (**s**) and triplet (**t**) ethynyl-X-germylene ($\mathbf{2_{s\text{-}x}}$ and $\mathbf{2_{t\text{-}x}}$), at two levels of theory: first line, B3LYP/6-311++G**; second line, *MP2/6-311++G** in italics* (where X = H, F, Cl, and Br)

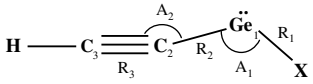

2

Structure/symmetry	Bond distances (Å)			Bond angles (°)	
	R_1	R_2	R_3	A_1	A_2
$\mathbf{2_{s\text{-}H}}(C_s)$	1.59	1.94	1.22	92.8	171.8
	1.58	*1.94*	*1.23*	*93.5*	*170.8*
$\mathbf{2_{s\text{-}F}}(C_s)$	1.80	1.96	1.21	96.7	170.3
	1.81	*1.95*	*1.23*	*96.3*	*169.9*
$\mathbf{2_{s\text{-}Cl}}(C_s)$	2.23	1.95	1.21	97.5	170.1
	2.19	*1.94*	*1.23*	*97.2*	*168.5*
$\mathbf{2_{s\text{-}Br}}(C_s)$	2.39	1.95	1.21	97.7	170.1
	2.36	*1.94*	*1.23*	*97.2*	*168.6*
$\mathbf{2_{t\text{-}H}}$ (Cs)	1.54	1.87	1.22	118.3	173.2
	1.53	*1.92*	*1.19*	*117.1*	*175.9*
$\mathbf{2_{t\text{-}F}}(C_s)$	1.78	1.86	1.22	117.5	173.0
	1.79	*1.91*	*1.20*	*114.5*	*172.4*
$\mathbf{2_{t\text{-}Cl}}(C_s)$	2.19	1.86	1.22	118.5	172.1
	2.16	*1.91*	*1.20*	*116.2*	*173.6*
$\mathbf{2_{t\text{-}Br}}(C_s)$	2.35	1.87	1.22	119.1	173.1
	2.31	*1.92*	*1.20*	*117.1*	*173.5*

2.2. Relative energies of isomers

The relative energy of C_2GeH_2 isomers, calculated at CCSD(T)/6-311++G** is: $\mathbf{1_{s\text{-}H}}$ (0.00 kcal/mol) > $\mathbf{3_{s\text{-}H}}$ (11.91 kcal/mol) > $\mathbf{2_{s\text{-}H}}$ (16.94 kcal/mol) > $\mathbf{2_{t\text{-}H}}$ (35.02 kcal/mol) > $\mathbf{1_{t\text{-}H}}$ (40.8 kcal/mol) > $\mathbf{3_{t\text{-}H}}$ (46.73 kcal/mol) (Table 1). The structure of lowest energy (global minimum) among the C_2GeH_2 isomers appears as singlet germacyclopropenylidene, $\mathbf{1_{s\text{-}H}}$; which is in agreement with the previously reported results related to carbenic C_3HX, C_3HY, C_2PX, and C_2NY as well as silylenic CNSiX, and C_2HSiX systems (where Y = NH_2, OMe, and CN) [21–26]. One may justify the above trend by considering the aromatic character of $\mathbf{1_{s\text{-}H}}$, caused by incorporating a σ^2 Ge center, making the π^2 of C_2–C_3 delocalize through the empty p-orbital on Ge (Fig. 5).

In order to estimate the extent of aromaticity of the cyclic species NICS method is employed. NICS is a computational method which provides an indirect theoretical probe of ring currents to serve as an aromaticity criterion [39]. The NICS indices are based on the "absolute magnetic shielding" taken at the center of a ring compound, where the full effect of the induced ring current should be observed. Also, NICS (1) (i.e., at points 1 Å above the ring center) was suggested to be a better measure of the π electron delocalization, compared to NICS(0) (i.e., at the ring center) [44]. The calculated NICS indices with negative values are aromatic, and those with positive values are anti-

Table 8
Optimized geometrical parameters (bond distances (R) and bond angles (A)) along with symmetry, for singlet (**s**) and triplet (**t**) X-vinilydenegermylene ($\mathbf{3_{s\text{-}x}}$ and $\mathbf{3_{t\text{-}x}}$), at two levels of theory: first line, B3LYP/6-311++G**; second line, *MP2/6-311++G** in italics* (where X = H, F, Cl, and Br)

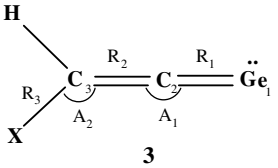

3

Structure/symmetry	Bond distances (Å)			Bond angles (°)	
	R_1	R_2	R_3	A_1	A_2
$\mathbf{3_{s\text{-}H}}(C_{2v})$	1.79	1.32	1.09	180.0	122.3
	1.79	*1.34*	*1.09*	*179.9*	*121.9*
$\mathbf{3_{s\text{-}F}}(C_s)$	1.77	1.32	1.36	178.7	123.2
	1.78	*1.33*	*1.35*	*176.2*	*122.9*
$\mathbf{3_{s\text{-}Cl}}(C_s)$	1.78	1.31	1.78	177.9	124.1
	1.79	*1.33*	*1.74*	*176.4*	*123.9*
$\mathbf{3_{s\text{-}Br}}(C_s)$	1.78	1.31	1.96	178.0	124.0
	1.79	*1.33*	*1.92*	*177.5*	*123.5*
$\mathbf{3_{t\text{-}H}}(C_{2v})$	1.89	1.31	1.09	179.9	121.6
	1.93	*1.30*	*1.09*	*180.0*	*121.4*
$\mathbf{3_{t\text{-}F}}(C_s)$	1.90	1.32	1.36	179.6	122.1
	1.95	*1.30*	*1.35*	*179.6*	*123.2*
$\mathbf{3_{t\text{-}Cl}}(C_s)$	1.89	1.32	1.78	179.1	121.8
	1.94	*1.30*	*1.75*	*179.8*	*122.9*
$\mathbf{3_{t\text{-}Br}}(C_s)$	1.90	1.31	1.94	178.4	120.1
	1.94	*1.30*	*1.92*	*179.3*	*120.9*

Table 9
Optimized geometrical parameters (bond distances (R) and bond angles (A)) along with symmetry, for singlet (**s**) and triplet (**t**) (X-ethynyl)germylene ($\mathbf{4_{s\text{-}x}}$ and $\mathbf{4_{t\text{-}x}}$), at two levels of theory: first line, B3LYP/6-311++G**; second line, *MP2/6-311++G** in italics* (where X = H, F, Cl, and Br)

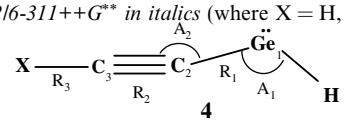

4

Structure/symmetry	Bond distances (Å)			Bond angles (°)	
	R_1	R_2	R_3	A_1	A_2
$\mathbf{4_{s\text{-}F}}(C_s)$	1.94	1.21	1.28	92.9	171.4
	1.97	*1.23*	*1.28*	*93.7*	*168.1*
$\mathbf{4_{s\text{-}Cl}}(C_s)$	1.93	1.22	1.64	92.9	170.2
	1.94	*1.24*	*1.64*	*93.8*	*165.9*
$\mathbf{4_{s\text{-}Br}}(C_s)$	1.93	1.22	1.79	92.8	170.9
	1.94	*1.24*	*1.79*	*93.7*	*167.1*
$\mathbf{4_{t\text{-}F}}(C_s)$	1.87	1.21	1.28	117.7	172.3
	1.91	*1.20*	*1.28*	*118.1*	*176.6*
$\mathbf{4_{t\text{-}Cl}}(C_s)$	1.86	1.22	1.64	117.8	170.3
	1.91	*1.20*	*1.64*	*117.1*	*172.9*
$\mathbf{4_{t\text{-}Br}}(C_s)$	1.86	1.22	1.79	117.7	170.6
	1.91	*1.19*	*1.79*	*117.1*	*174.2*

Table 10
NBO analyses including atomic charges and bond orders of C_2GeHX germylenes, **1**–**4**, calculated at B3LYP/6-311++G** (X = H, F, Cl, and Br)

Structure	Atomic charge					Bond order				
	Ge	C_2	C_3	H	X	Ge–C_2	Ge–C_3	C_2–C_3	C_2–X	C_3–H
$\mathbf{1_{s\text{-}H}}$	0.73	−0.57	−0.57	0.20	0.20	1.05	1.05	1.93	1.00	1.00
$\mathbf{1_{t\text{-}H}}$	0.14	−0.31	−0.33	0.25	0.25	–	–	–	–	–
$\mathbf{1_{s\text{-}F}}$	0.75	0.01	−0.63	0.22	−0.34	1.00	1.01	1.90	0.90	0.99
$\mathbf{1_{t\text{-}F}}$	0.50	−0.16	−0.19	0.21	−0.35	0.99	0.36	2.10	0.89	1.00
$\mathbf{1_{s\text{-}Cl}}$	0.81	−0.49	−0.57	0.22	0.03	–	–	–	–	–
$\mathbf{1_{t\text{-}Cl}}$	0.33	−0.18	−0.55	0.25	0.14	0.61	0.79	2.28	1.33	0.99
$\mathbf{1_{s\text{-}Br}}$	0.83	−0.57	−0.56	0.22	0.09	1.02	0.99	1.96	1.22	0.99
$\mathbf{1_{t\text{-}Br}}$	0.51	−0.52	−0.13	0.23	−0.10	0.93	0.17	2.49	0.53	1.00
						Ge–C_2	C_2–C_3	C_3–H	Ge–X	
$\mathbf{2_{s\text{-}H}}$	0.77	−0.56	−0.17	0.22	−0.26	0.92	2.76	1.01	0.89	
$\mathbf{2_{t\text{-}H}}$	0.60	−0.55	−0.16	0.23	−0.11	1.16	2.74	1.01	1.04	
$\mathbf{2_{s\text{-}F}}$	1.22	−0.62	−0.15	0.22	−0.67	0.85	2.76	1.00	0.81	
$\mathbf{2_{t\text{-}F}}$	1.11	−0.60	−0.14	0.23	−0.61	1.23	2.77	1.00	0.89	
$\mathbf{2_{s\text{-}Cl}}$	0.96	−0.59	−0.14	0.22	−0.45	0.88	2.76	1.00	0.99	
$\mathbf{2_{t\text{-}Cl}}$	0.81	−0.56	−0.14	0.23	−0.33	1.21	2.76	1.00	1.13	
$\mathbf{2_{s\text{-}Br}}$	0.89	−0.59	−0.15	0.23	−0.38	0.89	2.75	1.00	1.05	
$\mathbf{2_{t\text{-}Br}}$	0.72	−0.56	−0.15	0.23	−0.24	1.19	2.75	1.00	1.20	
						Ge–C_2	C_2–C_3	C_3–X	C_3–H	
$\mathbf{3_{s\text{-}H}}$	0.73	−0.81	−0.31	0.19	0.19	1.80	1.91	0.98	0.98	
$\mathbf{3_{t\text{-}H}}$	−0.26	−0.53	−0.39	0.09	0.09	1.46	2.00	0.96	0.96	
$\mathbf{3_{s\text{-}F}}$	0.84	−0.96	0.31	0.17	−0.35	1.72	1.88	0.88	0.95	
$\mathbf{3_{t\text{-}F}}$	−0.20	−0.61	−0.07	0.08	−0.20	1.33	1.93	0.87	0.95	
$\mathbf{3_{s\text{-}Cl}}$	0.83	−0.87	−0.14	0.21	−0.02	1.70	1.94	1.15	0.97	
$\mathbf{3_{t\text{-}Cl}}$	−0.19	−0.57	−0.29	0.10	−0.05	1.37	1.98	1.14	0.96	
$\mathbf{3_{s\text{-}Br}}$	0.83	−0.87	−0.20	0.21	0.02	1.68	1.96	1.18	0.97	
$\mathbf{3_{t\text{-}Br}}$	0.57	−0.44	−0.42	0.24	0.06	1.37	2.01	1.14	0.97	
						Ge–C_2	C_2–C_3	C_3–X	Ge–H	
$\mathbf{4_{s\text{-}F}}$	0.77	−0.70	0.46	−0.27	−0.26	–	–	–	–	
$\mathbf{4_{t\text{-}F}}$	0.58	−0.67	0.46	−0.11	−0.26	1.11	2.58	0.93	1.04	
$\mathbf{4_{s\text{-}Cl}}$	0.77	−0.56	−0.10	−0.26	0.15	0.91	2.67	1.33	0.89	
$\mathbf{4_{t\text{-}Cl}}$	0.59	−0.55	−0.09	−0.11	0.16	1.16	2.66	1.34	1.04	
$\mathbf{4_{s\text{-}Br}}$	0.77	−0.55	−0.19	−0.26	0.23	0.91	2.71	1.37	0.89	
$\mathbf{4_{t\text{-}Br}}$	0.59	−0.54	−0.18	−0.11	0.24	1.16	2.70	1.38	1.04	

aromatic. Our calculated NICS values indicate that all singlet cyclic germylenes, $\mathbf{1_{s\text{-}X}}$, show aromatic character with negative NICS values (Table 5). The aromatic characters of $\mathbf{1_{s\text{-}X}}$ are less than those of singlet cyclopropenylidene (NICS(1) = −17.07 ppm), cyclopropenyl cation (NICS(1) = −14.69 ppm), but higher than that of benzene ring (NICS(1) = −10.6 ppm) [44,45]. Moreover, based on calculated NICS values for germacyclopropenyl cation (C_2GeH_3-three member cyclic structure); this cation is less aromatic than the $\mathbf{1_{s\text{-}X}}$ germylenes (Table 5). Halogens appear to somewhat decrease the aromaticity of singlet germylenes $\mathbf{1_{s\text{-}X}}$. Since, change in NICS values is often translated into considerable aromatic and thereby stabilization differences. For example, judging from NICS(2.0) values, a di-*tert*-butylaminosilylene (−2.7 ppm) is reported to be significantly less aromatic than benzene (−5.3 ppm) [46]. $\mathbf{3_{s\text{-}H}}$ is less stable than $\mathbf{1_{s\text{-}H}}$, as indicated by the lack of aromatic character (Table 1). The stabilizing affects of an additional Ge–C bond in $\mathbf{3_{s\text{-}H}}$, as a replacement for Ge–H bond in $\mathbf{2_{s\text{-}H}}$, makes the former more stable than the latter. $\mathbf{3_{t\text{-}H}}$ is the most stable triplet isomer in C_2GeH_2 germylenes, which in turn is less stable that $\mathbf{2_{s\text{-}H}}$. An allylic resonance hybrid contributor justifies higher stability of $\mathbf{3_{t\text{-}H}}$ over $\mathbf{2_{t\text{-}H}}$. Moreover, a less significant vinylic resonance hybrid contributor indicates the lower resonance role in stabilizing $\mathbf{2_{t\text{-}H}}$ compared to $\mathbf{3_{t\text{-}H}}$. Finally, due to the considerable angle strains, cyclic $\mathbf{1_{t\text{-}H}}$ turns out to be a very unstable isomer in the C_2GeH_2 series.

The CCSD(T)/6-311++G** calculated relative stability of C_2GeHF species is: $\mathbf{2_{s\text{-}F}}$ (0.00 kcal/mol) > $\mathbf{1_{s\text{-}F}}$ (24.24 kcal/mol) > $\mathbf{3_{s\text{-}F}}$ (32.56 kcal/mol) > $\mathbf{2_{t\text{-}F}}$ (53.9 kcal/mol) > $\mathbf{4_{s\text{-}F}}$ (90.15 kcal/mol) > $\mathbf{4_{t\text{-}F}}$ (120.4 kcal/mol) > $\mathbf{3_{t\text{-}F}}$ (139.5 kcal/mol) (Table 2). Obviously, the stability order of C_2GeHF appears quite different from that of C_2GeH_2, and is in clear contrast to analogous C_3HF carbenes [21]. The global minimum for the set of C_2GeHF switches to singlet ethynylfluorogermylene, $\mathbf{2_{s\text{-}F}}$; which is highly stabilized by the electronegative fluorine atom directly attached to the divalent center [26]. Such a phenomenon apparently has more stabilizing effect than the aromaticity anticipated in $\mathbf{1_{s\text{-}F}}$ (Table 5). Nevertheless, aromaticity may justify the higher stability of $\mathbf{1_{s\text{-}F}}$ over $\mathbf{3_{s\text{-}F}}$. In turn, $\mathbf{3_{s\text{-}F}}$, being a singlet state germylene, is more stabilized by the electron-withdrawing fluorine, than $\mathbf{2_{t\text{-}F}}$ which is a triplet germylene.

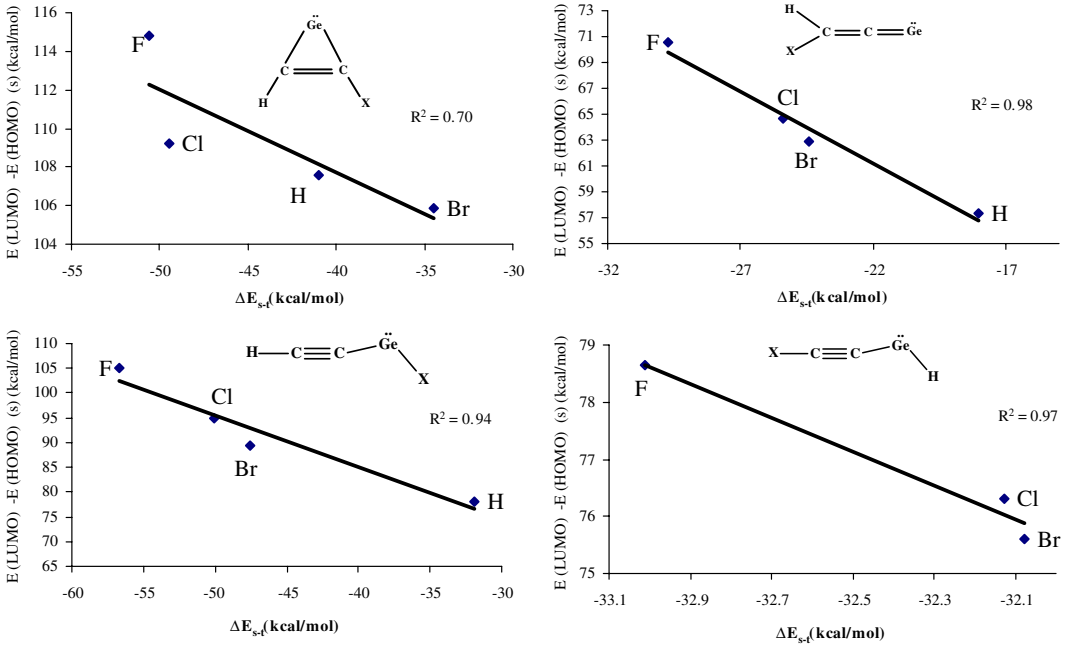

Fig. 2. Correlations between the LUMO–HOMO energy gaps of the singlet C_2GeHX germylenes ($\mathbf{1}_{s\text{-}X}$, $\mathbf{2}_{s\text{-}X}$, $\mathbf{3}_{s\text{-}X}$ and $^{a}\mathbf{4}_{s\text{-}X}$), and their corresponding singlet–triplet energy separations, $\Delta E_{s\text{-}t}$, for X = H, F, Cl, and Br calculated at B3LYP/6-311++G** (R^2 is the correlation coefficient); ^{a}For $\mathbf{4}_{s\text{-}X}$ data for X = H are not included.

The latter appears more stable than $\mathbf{4}_{s\text{-}F}$. Hence, fluorine attached to the C≡C in $\mathbf{4}_{s\text{-}F}$ fails to show much of stabilizing effect on germylenic center. Singlet $\mathbf{4}_{s\text{-}F}$ appears more stable than the triplet states $\mathbf{4}_{t\text{-}F}$ and $\mathbf{3}_{t\text{-}F}$. Finally, $\mathbf{1}_{t\text{-}F}$ is a transition state on the potential energy surface of C_2GeHF (Table 2). The CCSD(T)/6-311++G** calculated relative stability order for the isomers of C_2GeHCl is: $\mathbf{2}_{s\text{-}Cl}$ (0.00 kcal/mol) > $\mathbf{1}_{s\text{-}Cl}$ (21.46 kcal/mol) > $\mathbf{3}_{s\text{-}Cl}$ (33.17 kcal/mol) > $\mathbf{4}_{s\text{-}Cl}$ (46.79 kcal/mol) > $\mathbf{2}_{t\text{-}Cl}$ (47.39 kcal/mol) > $\mathbf{3}_{t\text{-}Cl}$ (61.99 kcal/mol) > $\mathbf{1}_{t\text{-}Cl}$ (72.76 kcal/mol) > $\mathbf{4}_{t\text{-}Cl}$ (77.30 kcal/mol) (Table 3). This is nearly the same trend found for C_2GeHF, but with a shorter range of energy differences between the isomers involved; due to lower stabilizing effect of chlorine, than fluorine, on the singlet states. The same justifications for the relative stability of C_2GeHF may be applied to C_2GeHCl [26]. The global minimum for the set of C_2GeHCl appears to be singlet ethynylchlorogermylene, $\mathbf{2}_{s\text{-}Cl}$.

The CCSD(T)/6-311++G** calculated relative stability of C_2GeHBr isomers is: $\mathbf{2}_{s\text{-}Br}$ (0.00 kcal/mol) > $\mathbf{1}_{s\text{-}Br}$ (22.91 kcal/mol) > $\mathbf{3}_{s\text{-}Br}$ (35.23 kcal/mol) > $\mathbf{2}_{t\text{-}Br}$ (45.4 kcal/mol) > $\mathbf{4}_{s\text{-}Br}$ (48.4 kcal/mol) > $\mathbf{3}_{t\text{-}Br}$ (62.61 kcal/mol) > $\mathbf{1}_{t\text{-}Br}$ (73.28 kcal/mol) > $\mathbf{4}_{t\text{-}Br}$ (78.81 kcal/mol) (Table 4). Again, this is the same trend found for both C_2GeHF and C_2GeHCl. Interestingly, the range of energy differences between C_2GeHCl and C_2GeHBr is similar. This finding indicates that both the electro-negativity as well as the resonance effects of the halogen atoms is important for the stabilization of germylenic centers [47]. Again, the global minimum for the set of C_2GeHBr appears to be singlet $\mathbf{2}_{s\text{-}Br}$. Resonance effects of halogens are dissimilar on different structures. Inspection of halogen–carbon or halogen–germanium bond orders indicate that halogen–carbon bond orders vary between 0.53 ($\mathbf{1}_{t\text{-}Br}$) to 1.38 ($\mathbf{4}_{t\text{-}Br}$). Halogen–germanium bond orders vary between 0.81 ($\mathbf{2}_{s\text{-}F}$) to 1.2 ($\mathbf{2}_{t\text{-}Br}$) (Table 10).

2.3. Singlet–triplet, HOMO–LUMO, energy separations

This section starts with the examination of cyclic germylenes $\mathbf{1}_{s\text{-}X}$ and $\mathbf{1}_{t\text{-}X}$. The CCSD(T)/6-311++G** calculated order of singlet–triplet energy gaps ($\Delta E_{s\text{-}t,X}$), between $\mathbf{1}_{s\text{-}X}$ and $\mathbf{1}_{t\text{-}X}$ isomers is: $\Delta E_{s\text{-}t,Cl}$ (51.30 kcal/mol) > $\Delta E_{s\text{-}t,Br}$ (50.37 kcal/mol) > $\Delta E_{s\text{-}t,H}$ (40.80 kcal/mol). Excluding the fluorine which has a transition state structure for $\mathbf{1}_{t\text{-}F}$, chlorine shows the highest stabilizing effect on the singlet states among cyclic $\mathbf{1}_{s\text{-}X}$. This is in contrast to the case of C_2SiHX silylenes, where hydrogen had the highest $\Delta E_{s\text{-}t,X}$. When X = Cl and/or Br; variations between their corresponding $\Delta E_{s\text{-}t,X}$ is little, since in cyclic species $\mathbf{1}_{s\text{-}X}$ and $\mathbf{1}_{t\text{-}X}$, the halogen atoms are not directly bonded to the divalent center (Fig. 1).

Ethynylgermylene (**2**) is the most energetically feasible acyclic structure investigated (Fig. 1). **2** is more affected by halogens than **1**, **3**, or **4** due to the direct attachment of the halogens to its divalent center. Singlet states $\mathbf{2}_{s\text{-}x}$ (X = H, F, Cl, and Br) are more stable than their corresponding $\mathbf{2}_{t\text{-}X}$. The CCSD(T)/6-311++G** calculated order of $\Delta E_{s\text{-}t,X}$, between $\mathbf{2}_{s\text{-}X}$ and $\mathbf{2}_{t\text{-}X}$ is: $\Delta E_{s\text{-}t,F}$ (53.90 kcal/mol) > $\Delta E_{s\text{-}t,Cl}$ (47.39 kcal/mol) > $\Delta E_{s\text{-}t,Br}$ (45.40 kcal/mol) > $\Delta E_{s\text{-}t,H}$ (29.79 kcal/mol) (Tables 1–4). Again, this finding clearly demonstrates the stabilizing of germylenes, due to the effect of electronegativity [1]. Among all the halogenated structures studied, acyclic singlet $\mathbf{2}_{s\text{-}X}$ appears as

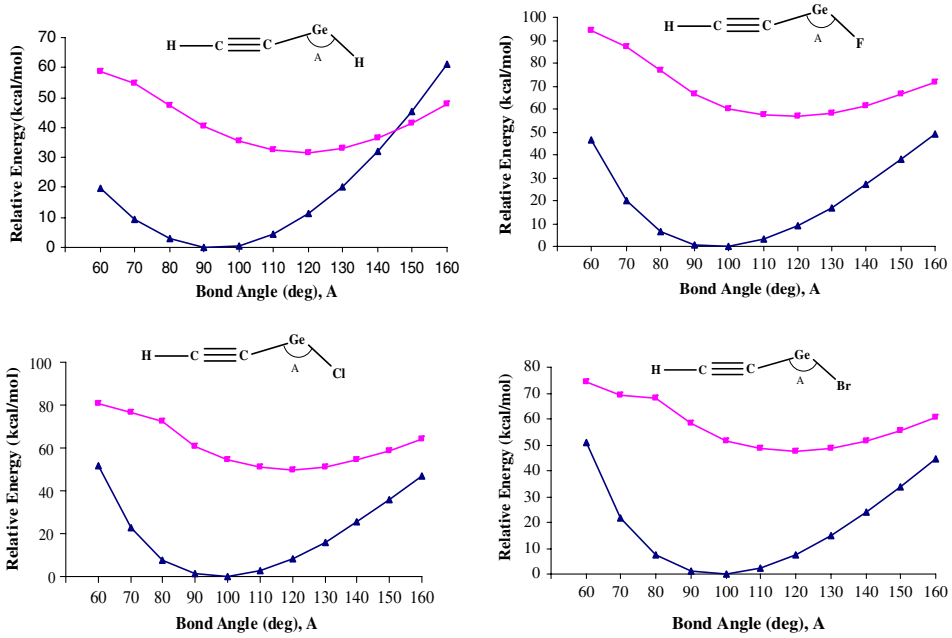

Fig. 3. Bending potential energy curves (relative energies as a function of the divalent bond angle, A) of the singlet (**s**, ▲) and triplet (**t**, ■) states of ethynyl-X-germylene, $\mathbf{2}_{\mathbf{s\text{-}X}}$ and $\mathbf{2}_{\mathbf{t\text{-}X}}$ (X = H, F, Cl, and Br).

the global minima, in agreement with the C_2SiHX silylenes, which was previously reported [26]. The magnitude of divalent bond angle is one of the most significant parameters, predicted to affect $\Delta E_{s\text{-}t}$ and/or the choice of electronic ground states of the divalent group 14 species [48]. Bending potential energy curves for $\mathbf{2}_{\mathbf{s\text{-}X}}$ and $\mathbf{2}_{\mathbf{t\text{-}X}}$, calculated with B3LYP/6-311++G**, show the crossing of singlet $\mathbf{2}_{\mathbf{s\text{-}X}}$ and triplet states $\mathbf{2}_{\mathbf{t\text{-}X}}$ curves, for only X = H, with a ∠XGeC divalent angle of 146° (Fig. 3). In contrast, for X = F, Cl, and Br, the singlet states appear more stable than their corresponding triplet states, regardless of the employed angle ∠XGeC. This is possibly due to the stabilizing effects of halogens (X) on the singlet divalent centers [49]. Atomic charges on divalent Ge atoms appear linearly correlated with the Swain and Lupton resonance constants (R) [50], for both acyclic germylenes $\mathbf{2}_{\mathbf{s\text{-}X}}$ and $\mathbf{2}_{\mathbf{t\text{-}X}}$ (Fig. 4).

Another acyclic structure considered is vinylidengermylene (**3**) (Fig. 1). All calculations reveal that singlet states $\mathbf{3}_{\mathbf{s\text{-}x}}$ are more stable than their corresponding triplet states $\mathbf{3}_{\mathbf{t\text{-}X}}$ (Tables 1–4). The order of $\Delta E_{s\text{-}t}$ between $\mathbf{3}_{\mathbf{s\text{-}X}}$ and $\mathbf{3}_{\mathbf{t\text{-}X}}$, calculated at CCSD(T)/6-311++G**, follows the electronegativity of X: $\Delta E_{\mathbf{s\text{-}t,F}}$ (106.93 kcal/mol) > $\Delta E_{\mathbf{s\text{-}t,Cl}}$ (28.82 kcal/mol) > $\Delta E_{\mathbf{s\text{-}t,Br}}$ (27.37 kcal/mol) > $\Delta E_{\mathbf{s\text{-}t,H}}$ (23.11 kcal/mol).

The last acyclic structure considered is (X-ethynyl)germylene, **4** (Fig. 1). This structure is closely related to structure **2**; besides, when X = H, structure **4** becomes exactly the same as structure **2**. Every $\mathbf{4}_{\mathbf{s\text{-}x}}$ and/or $\mathbf{4}_{\mathbf{t\text{-}x}}$ is less stable than its corresponding $\mathbf{2}_{\mathbf{s\text{-}x}}$ and/or $\mathbf{2}_{\mathbf{t\text{-}x}}$. Again, all singlet states $\mathbf{4}_{\mathbf{s\text{-}x}}$ appear more stable than their corresponding triplet states $\mathbf{4}_{\mathbf{t\text{-}x}}$. The magnitudes of $\Delta E_{\mathbf{s\text{-}t,X}}$ between $\mathbf{4}_{\mathbf{s\text{-}X}}$ and $\mathbf{4}_{\mathbf{t\text{-}X}}$, calculated at CCSD(T)/6-311++G**, are nearly similar: $\Delta E_{\mathbf{s\text{-}t,F}}$ (30.26 kcal/mol) ≈ $\Delta E_{\mathbf{s\text{-}t,Cl}}$ (30.52 kcal/mol) ≈ $\Delta E_{\mathbf{s\text{-}t,Br}}$ (30.54 kcal/mol) (Tables 2–4).

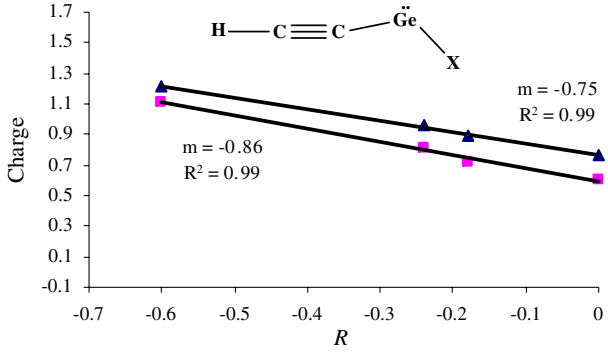

Fig. 4. Plots of atomic charges on the divalent center vs. resonance (R) (Swain and Lupton constants [50]) for singlet (▲) and triplet (■) states of ethynyl-X-germylene, $\mathbf{2}_{\mathbf{s\text{-}X}}$ and $\mathbf{2}_{\mathbf{t\text{-}X}}$, where X = H, F, Cl, and Br (R^2 = correlation coefficient, m = curve slope).

2.4. Geometries, dipole moments, and atomic charges

During optimization, structures of cyclic triplet states $\mathbf{1}_{\mathbf{t\text{-}H}}$ (MP2/6-311++G**), $\mathbf{1}_{\mathbf{t\text{-}F}}$ (B3LYP/6-311++G**) and $\mathbf{1}_{\mathbf{t\text{-}Br}}$ (B3LYP/6-311++G**) transform into their corresponding acyclic structures, due to the angle strains involved (Tables 6–9). At MP2/6-311++G** optimization, both C_2–Ge and C_3–Ge bonds of $\mathbf{1}_{\mathbf{t\text{-}H}}$ cleave to form an acetylenic acyclic structure (neither **2** nor **4**). While, at B3LYP/6-311++G** optimization, $\mathbf{1}_{\mathbf{t\text{-}F}}$ rearranges to an acyclic structure with Br atom bonded to Ge. However, at B3LYP/6-311++G** optimization, just the C_3–Ge bond of $\mathbf{1}_{\mathbf{t\text{-}Br}}$ cleaves. The R_1 and R_3 bond lengths in $\mathbf{1}_{\mathbf{s\text{-}X}}$ structures are 0.30–0.35 Å shorter than those of $\mathbf{1}_{\mathbf{t\text{-}X}}$. In contrast, R_2 bond lengths in $\mathbf{1}_{\mathbf{s\text{-}X}}$ structures are about 0.10–0.13 Å longer than those of $\mathbf{1}_{\mathbf{t\text{-}X}}$ (Tables 6 and 10).

Table 11
NBO calculated bond hybridizations for singlet ($\mathbf{1_{s\text{-}X}}$ and $\mathbf{2_{s\text{-}X}}$) and triplet states ($\mathbf{1_{t\text{-}X}}$ and $\mathbf{2_{t\text{-}X}}$) of C_2GeHX germylenes as well as hybridizations for Ge lone-pairs (L) of singlet $\mathbf{1_{s\text{-}X}}$ (X = H, F, Cl, and Br)

Structure	Bond			Structure	Bond	
	σ_{Ge-C2}	σ_{Ge-C3}	Ge–L		σ_{Ge-C}	σ_{Ge-X}
$\mathbf{1_{s\text{-}H}}$	$s^1p^{13.15}d^{0.04}$	$s^1p^{13.15}d^{0.04}$	$s^1p^{0.13}d^{0.00}$	$\mathbf{2_{s\text{-}H}}$	$s^1p^{7.98}d^{0.05}$	$s^1p^{10.07}d^{0.05}$
$\mathbf{1_{t\text{-}H}}$	$s^1p^{67.85}d^{0.42}$	$s^1p^{68.45}d^{0.43}$	–	$\mathbf{2_{t\text{-}H}}$	$s^1p^{4.77}d^{0.02}$	$s^1p^{5.91}d^{0.01}$
$\mathbf{1_{s\text{-}F}}$	$s^1p^{14.59}d^{0.07}$	$s^1p^{13.64}d^{0.06}$	$s^1p^{0.13}d^{0.00}$	$\mathbf{2_{s\text{-}F}}$	$s^1p^{9.70}d^{0.08}$	$s^1p^{11.77}d^{0.08}$
$\mathbf{1_{t\text{-}F}}$	–	–	–	$\mathbf{2_{t\text{-}F}}$	$s^1p^{5.35}d^{0.03}$	$s^1p^{9.18}d^{0.05}$
$\mathbf{1_{s\text{-}Cl}}$	$s^1p^{13.90}d^{0.05}$	$s^1p^{14.28}d^{0.06}$	$s^1p^{0.14}d^{0.00}$	$\mathbf{2_{s\text{-}Cl}}$	$s^1p^{9.04}d^{0.08}$	$s^1p^{16.63}d^{0.24}$
$\mathbf{1_{t\text{-}Cl}}$	$s^1p^{99.99}d^{1.23}$	$s^1p^{22.43}d^{0.15}$	–	$\mathbf{2_{t\text{-}Cl}}$	$s^1p^{5.38}d^{0.03}$	$s^1p^{11.11}d^{0.12}$
$\mathbf{1_{s\text{-}Br}}$	$s^1p^{13.71}d^{0.05}$	$s^1p^{14.57}d^{0.06}$	$s^1p^{0.14}d^{0.00}$	$\mathbf{2_{s\text{-}Br}}$	$s^1p^{8.99}d^{0.07}$	$s^1p^{18.94}d^{0.02}$
$\mathbf{1_{t-Br}}$	–	–	–	$\mathbf{2_{t\text{-}Br}}$	$s^1p^{5.57}d^{0.03}$	$s^1p^{12.63}d^{0.10}$

The divalent bond angles $\angle A_1$ or $\angle CGeC$ in $\mathbf{1_{s\text{-}X}}$ are about 10° larger than their corresponding $\mathbf{1_{t\text{-}X}}$. This result is in contrast to the reported findings on acyclic germylenes and silylenes [47]. For instance, in the cyclic structures $\mathbf{1_{s\text{-}X}}$ and $\mathbf{1_{t\text{-}X}}$ the strictly localized natural bond orbitals (NBO) of the σ molecular orbitals have significant p character on divalent Ge centers (Table 11). Nevertheless, p character of Ge in $\mathbf{1_{t\text{-}X}}$ is greatly higher than those of $\mathbf{1_{s\text{-}X}}$ which cause the widening of divalent angle $\angle CGeC$ in cyclic singlet states $\mathbf{1_{s\text{-}X}}$, compared to the triplet states $\mathbf{1_{t\text{-}X}}$. This is in clear contrast to the case of acyclic structures $\mathbf{2_{s\text{-}X}}$ and $\mathbf{2_{t\text{-}X}}$, where divalent atoms Ge in $\mathbf{2_{s\text{-}X}}$ possess higher p character than $\mathbf{2_{t\text{-}X}}$ (Table 11). Consequently, divalent angles $\angle CGeX$ in $\mathbf{2_{s\text{-}X}}$ are smaller than those of the triplet $\mathbf{2_{t\text{-}X}}$. The lone pairs on Ge atom in $\mathbf{1_{s\text{-}X}}$ structures have mainly s character. Interestingly, only a little germanium d orbital valence participation is found for the cyclic triplet structures $\mathbf{1_{t\text{-}X}}$. 3D and 2D isosurface HOMO plots, obtained for $\mathbf{1_{s\text{-}Cl}}$ and $\mathbf{1_{t\text{-}Cl}}$, illustrate the $\sigma^2(A^1)$ configuration for HOMO of the $\mathbf{1_{s\text{-}Cl}}$ and partial participation of Ge d-orbitals with a lower looseness of electrons for HOMO of $\mathbf{1_{t\text{-}Cl}}$ (Fig. 5).

Unexpectedly, changes are small in geometrical parameters of acyclic structure **2**, where the X is directly attached to divalent center (Table 7). The changes in R_2 bond orders ($Ge–C_2$), as a function of X in $\mathbf{2_{s\text{-}X}}$ follow the trend: H > Br > Cl > F; while, the corresponding triplet $\mathbf{2_{t\text{-}X}}$ follows the opposite trend: F > Cl > Br > H. In

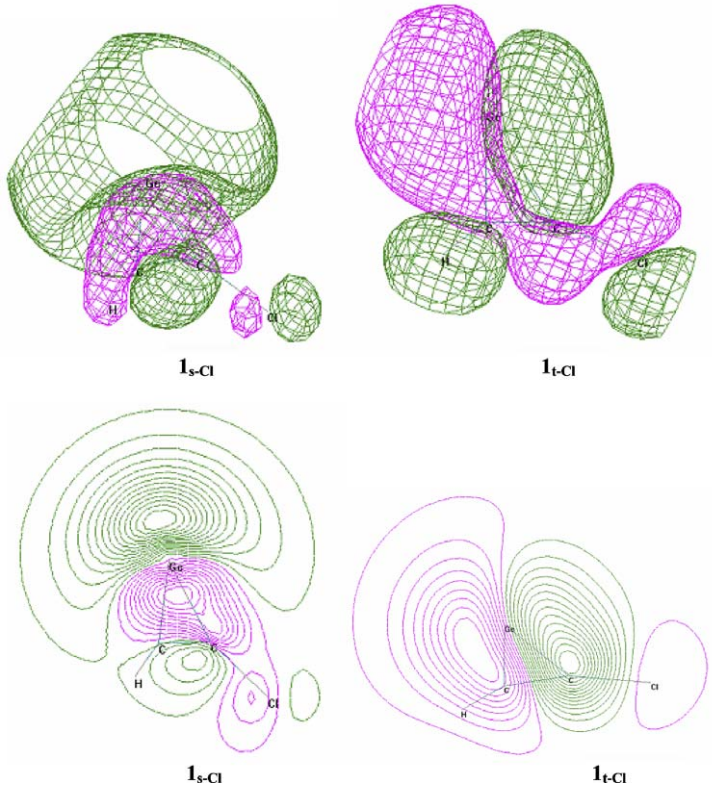

Fig. 5. Isosurface visualization of the HOMO molecular orbitals showing the contribution of Ge d-orbitals of singlet $\mathbf{1_{s\text{-}Cl}}$ and triplet $\mathbf{1_{t\text{-}Cl}}$ germylenes in 2D (bottom) and 3D (top) fashion.

addition, R_2 bond orders in all triplet states $\mathbf{2}_{\mathbf{t\text{-}X}}$ are larger than their corresponding singlet states $\mathbf{2}_{\mathbf{s\text{-}X}}$. Considering the intrinsic tendency of divalent Ge in acquiring stable singlet states [1,47–49], the canonical form H—C≡C—Ge—X appears to carry a higher relative weight for singlet states, $\mathbf{2}_{\mathbf{s\text{-}X}}$. In contrast, since the triplet state divalent Ge is rare, for being highly instable, the canonical form H—C=C=Ge=X turns out to carry a higher weight for triplet states, $\mathbf{2}_{\mathbf{t\text{-}X}}$. The calculated geometrical parameters and atomic charges emerge consistent with this argument. As expected for acyclic germylenes and silylenes, the divalent bond angles $\angle A_1$, in all singlet $\mathbf{2}_{\mathbf{s\text{-}X}}$ are about 20–30° smaller than their corresponding $\mathbf{2}_{\mathbf{t\text{-}X}}$ (Table 7). Although, $\mathbf{2}_{\mathbf{s\text{-}H}}$ and $\mathbf{2}_{\mathbf{t\text{-}H}}$ are nearly non-polar, with low dipole moments, their halogenated derivatives $\mathbf{2}_{\mathbf{s\text{-}X}}$ and/or $\mathbf{2}_{\mathbf{t\text{-}X}}$ have the highest dipole moments among **1**–**4** (Tables 1–4).

In structure **3**, the R_1 bond lengths of triplet $\mathbf{3}_{\mathbf{t\text{-}X}}$ are about 0.10–0.14 Å longer than their corresponding $\mathbf{3}_{\mathbf{s\text{-}X}}$. The changes in R_1 bond orders (Ge–C_2), as a function of X in $\mathbf{3}_{\mathbf{s\text{-}X}}$ follow the size: H > F > Cl > Br. However, the order of changes in R_2 bond orders (C_2–C_3), as a function of X is: Br > Cl > H > F. Replacing of H with X in both $\mathbf{3}_{\mathbf{s\text{-}X}}$ and $\mathbf{3}_{\mathbf{t\text{-}X}}$, cause to a little deviation (0.5–2°) from linearity of cumulenic moiety, C=C=Ge (Table 8).

The last acyclic structure considered is **4** which also show negligible change in their geometrical parameters as a function of X, regardless of the divalent bond angle $\angle A_1$. In all singlet states $\mathbf{4}_{\mathbf{s\text{-}X}}$, the magnitude of $\angle A_1$ are smaller than those of their corresponding $\mathbf{4}_{\mathbf{t\text{-}X}}$ (Table 9). Moreover, among the four structural sets scrutinized, (haloethynyl)germylenes, **4**, have the lowest dipole moments (Tables 1–4).

The results of NBO analysis for atomic charges reveal that the atomic charges on the divalent centers (Ge), of $\mathbf{2}_{\mathbf{s\text{-}X}}$ and $\mathbf{2}_{\mathbf{t\text{-}X}}$, appear to have linear relationships with the Swain and Lupton [50] resonance constants (R), assuming comparable weighting factors ($f \approx r \approx 1$) for X (Table 10, Fig. 3).

Switch of global minima from cyclic structure **1** (X = H) to acyclic structure **2** (X = halogen) is due to several reasons including the following. (1) Halogens (X) stabilize $\mathbf{2}_{\mathbf{s\text{-}X}}$, compared to $\mathbf{2}_{\mathbf{s\text{-}H}}$. This is through electron withdrawing effects, which increase the positive charge on Ge [1,47–49]. The trend appears to follow electronegativity: $\mathbf{1}_{\mathbf{s\text{-}F}}$ (1.22) > $\mathbf{2}_{\mathbf{s\text{-}Cl}}$ (0.96) > $\mathbf{2}_{\mathbf{s\text{-}Br}}$ (0.89) > $\mathbf{2}_{\mathbf{s\text{-}H}}$ (0.77) (Table 10). The consistently higher positive (charge) character on Ge, when X = F, Cl, and/or Br, compared to X = H, is further dispersed through resonance with the adjacent triple bond C≡C in $\mathbf{2}_{\mathbf{s\text{-}X}}$. (2) Halogens also act as electron pair donors and stabilize acyclic $\mathbf{2}_{\mathbf{s\text{-}Cl}}$ and $\mathbf{2}_{\mathbf{s\text{-}Br}}$ through resonance, making the bond order of Ge–Cl = 0.99 and Ge–Br = 1.05 (Table 10). These halo bonds are considerably shorter than Ge–H with a bond order of 0.89. (3) Finally, perturbation of aromaticity of cyclic $\mathbf{1}_{\mathbf{s\text{-}X}}$, through cross conjugation involving halogen and the three member ring, reduce the relative stability of $\mathbf{1}_{\mathbf{s\text{-}X}}$, compared to $\mathbf{2}_{\mathbf{s\text{-}X}}$ (Table 5).

3. Conclusion

Singlet–triplet energy separations ($\Delta E_{\mathbf{s\text{-}t,X}}$), and relative stabilities of 30 new germylenes C_2GeHX are compared quantitatively (X = H, F, Cl and Br). Eight levels of calculations are employed including: HF/6-311++G**, B3LYP/LANL2DZ, B1LYP/6-311++G**, B3LYP/6-311++G**, MP2/6-311++G**, MP4/6-311++G**, QCISD(T)/6-311+G**, and CCSD(T)/6-311++G**. The possible structures considered for each singlet (**s**) and triplet (**t**) C_2GeH-X, are: X-germacyclopropenylidene ($\mathbf{1}_{\mathbf{s\text{-}X}}$ and $\mathbf{1}_{\mathbf{t\text{-}X}}$), ethynyl-X-germylene ($\mathbf{2}_{\mathbf{s\text{-}X}}$ and $\mathbf{2}_{\mathbf{t\text{-}X}}$), X-vinylidengermylene ($\mathbf{3}_{\mathbf{s\text{-}X}}$ and $\mathbf{3}_{\mathbf{t\text{-}X}}$), or (X-ethynyl)germylene, ($\mathbf{4}_{\mathbf{s\text{-}X}}$ and $\mathbf{4}_{\mathbf{t\text{-}X}}$). All singlet germylenes studied are lower in energy than their corresponding triplet states. The global minimum among six isomers of C_2GeH-H appears to be cyclic $\mathbf{1}_{\mathbf{s\text{-}X}}$, nevertheless the global minima among 24 structures of C_2GeHF, C_2GeHCl and C_2GeHBr switch to acyclic $\mathbf{2}_{\mathbf{s\text{-}X}}$. Order of $\Delta E_{\mathbf{s\text{-}t,X}}$ for **1**–**3** as a function of X is: H > F > Cl > Br, while $\Delta E_{\mathbf{s\text{-}t,X}}$ for structure **4** has little changes as a function of X employed. LUMO–HOMO energy gaps of the singlet germylenes, show linear correlations to their corresponding singlet–triplet energy separations, calculated at B3LYP/6-311++G**. Very little germanium d orbital valence participation is found for the cyclic triplet structures $\mathbf{1}_{\mathbf{t\text{-}X}}$. Bending potential energy curves show the crossing of singlet, $\mathbf{2}_{\mathbf{s\text{-}H}}$, and its corresponding triplet, $\mathbf{2}_{\mathbf{t\text{-}H}}$, at ∠HGeC angle of 146°.

Acknowledgements

We acknowledge the useful discussion and hints of A. Ghaderi (Chemistry Department, Imam Hossein University). Special thanks to S. Souri, Kh. Didehban, S. Soleimani-Amiri, N. Jalalimanesh, M. Ghavami, F. Buazar, E. Vessally, S. Arshadi and A.R. Bekhradnia (Chemistry Department, Tarbiat Modarres University) for their cordial cooperation.

Appendix A. Supplementary data

Supplementary data associated with this article can be found, in the online version, at doi:10.1016/j.jorganchem.2006.02.038.

References

[1] P.P. Gaspar, in: M. JonesJr., R.A. Moss (Eds.), The Silylenes in Reactive Intermediates, vol. 1, Wiley, New York, 1978.
[2] M. Ishikawa, M. Kumada, Adv. Organomet. Chem. 19 (1981) 51.
[3] P. Riviere, A. Castel, J. Satgt, J. Am. Chem. Soc. 102 (1980) 5413.
[4] O.M. Nefedov, S.P. Kolesnikov, A.I. loffe, J. Organomet. Chem., Chem. Lib. 5 (1977) 181;
Organomet. Chem. Rev. 5 (1977) 181.
[5] B.O. Roosand, P.M. Siegbahn, J. Am. Chem. Soc. 99 (1977) 7716.
[6] C.W. Bauschlicher, H.F. Schaefer III, P.S. Bagus, J. Am. Chem. Soc. 99 (1977) 7106.
[7] J.W. Kenney, J. Simons, G.D. Purvis, R.J. Bartlett, J. Am. Chem. Soc. 100 (1978) 6930.

[8] B. Wirsam, Chem. Phys. Lett. 14 (1972) 214.
[9] J.H. Meadows, H.F. Schaefer III, J. Am. Chem. Soc. 98 (1976) 4383.
[10] M.M. Heaton, J. Chem. Phys. 67 (1977) 5396.
[11] B. Wirsam, Chem. Phys. Lett. 22 (1973) 360.
[12] C. Thomson, Theor. Chim. Acta 32 (1973) 93.
[13] J.C. Barthelat, B.S. Roch, G. Trinquier, J. Satge, J. Am. Chem. Soc. 102 (1980) 4080.
[14] A. Selmani, D.R. Salahub, J. Chem. Phys. 89 (1988) 1529.
[15] H. Huber, E.P. Kundlg, G.A. Orin, A. Vandervoet, Can. J. Chem. 52 (1974) 95.
[16] J.L. Margrave, D.L. Perry, Inorg. Chem. 16 (1977) 820.
[17] C. Boehme, G. Frenking, J. Am. Chem. Soc. 118 (1996) 2039.
[18] W. Kutzelnigg, Angew. Chem., Int. Ed. 23 (1984) 272.
[19] A. Gobbi, G. Frenking, J. Am. Chem. Soc. 116 (1994) 9287.
[20] A.J. Arduengo III, H. Bock, H. Chen, M. Denk, D.A. Dixon, J.C. Green, W.A. Herrmann, N.L. Jones, M. Wagner, R. West, J. Am. Chem. Soc. 116 (1994) 6641.
[21] M.Z. Kassaee, B.N. Haerizade, S. Arshadi, J. Mol. Struct. (Theochem) 639 (2003) 187.
[22] M.Z. Kassaee, B.N. Haerizade, Z. Hossaini, J. Mol. Struct. (Theochem) 681 (2004) 129.
[23] M.Z. Kassaee, S.M. Musavi, M. Ghambarian, F. Buazar, J. Mol. Struct. (Theochem) 726 (2005) 171.
[24] M.Z. Kassaee, S.M. Musavi, F. Buazar, J. Mol. Struct. (Theochem) 728 (2005) 15.
[25] M.Z. Kassaee, S.M. Musavi, H. Hamadi, M. Ghambarian, S.E. Hosseini, J. Mol. Struct. (Theochem) 730 (2005) 33.
[26] M.Z. Kassaee, S.M. Musavi, F. Buazar, M. Ghambarian, J. Mol. Struct. (Theochem) 722 (2005) 151.
[27] M.J. Frisch, G.W. Trucks, H.B. Schlegel, G.E. Scuseria, M.A. Robb, J.R. Cheeseman, V.G. Zakrzewski Jr., J.A. Montgomery, R.E. Stratmann, J.C. Burant, S. Dapprich, J.M. Millan, A.D. Daniels, K.N. Kudin, M.C. Strain, O. Farkas, J. Tomasi, V. Barone, M. Cossi, R. Cammi, B. Mennucci, C. Pomelly, C. Adamo, S. Clifford, J. Ochterski, G.A. Petersson, P.Y. Ayala, Q. Cui, K. Morokuma, D.K. Malick, A.D. Rabuck, K. Raghavachari, J.B. Foresman, J. Cioslowski, J.V. Ortiz, A.G. Baboul, B.B. Stefanov, G. Liu, A. Liashenko, P. Piskorz, I. Komaromi, R. Gomperts, R.L. Martin, D.J. Fox, T. Keith, M.A. Al-Laham, C.Y. Peng, A. Nanayakkara, C. Gonzalez, M. Challacombe, P.M.W. Gill, B. Johnson, W. Chen, M.W. Wong, J.L. Andres, C. Gonzalez, M. Head-Gordon, E.S. Replogle, J.A. Pople, Gaussian 98, Revision A.7, Gaussian Inc., Pittsburgh, PA, 1998.
[28] A.D. Becke, J. Chem. Phys. 104 (1996) 1040.
[29] C. Adamo, V. Barone, Chem. Phys. Lett. 274 (1997) 242.
[30] P.J. Hay, W.R. Wadt, J. Chem. Phys. 82 (1985) 299.
[31] S. Saebo, J. Almlof, Chem. Phys. Lett. 154 (1989) 83.
[32] J.A. Pople, R. Krishnan, Int. J. Quant. Chem. 14 (1978) 91.
[33] R. Krishnan, M.J. Frisch, J.A. Pople, J. Chem. Phys. 72 (1980) 4244.
[34] J.A. Pople, M. Head-Gordon, K. Raghavachari, J. Chem. Phys. 87 (1987) 5968.
[35] G.E. Scuseria, H.F. Schaefer III, J. Chem. Phys. 90 (1989) 3700.
[36] R.F. Hout, B.A. Levi, W.J. Heher, J. Comput. Chem. 82 (1985) 234.
[37] D.J. Defrees, A.D. McLean, J. Chem. Phys. 82 (1985) 333.
[38] J.E. Carpenter, F. Weinhold, J. Mol. Struct. (Theochem) 41 (1988) 169.
[39] P.v.R. Schleyer, C. Maerker, A. Dransfeld, H. Jiao, N.J.R.v.E. Hommes, J. Am. Chem. Soc. 118 (1996) 6317.
[40] D.B. Chesnut, K.D. Moore, J. Comput. Chem. 10 (1985) 648.
[41] K. Wolinski, J.F. Hinton, P. Pulay, J. Am. Chem. Soc. 112 (1990) 8251.
[42] C. Barrientos, P. Redondo, A. Largo, J. Phys. Chem. A 104 (2000) 11541.
[43] C. Barrientos, A. Cimas, A. Largo, J. Phys. Chem. A 105 (2001) 6724.
[44] P.v.R. Schleyer, M. Manoharan, Z.X. Wang, B. Kiran, H. Jiao, R. Puchta, N.J.R.v.E. Hommes, Org. Lett. 3 (2001) 2465.
[45] M.N. Glukhovtsev, L. Sergei, P. Addy, J. Phys. Chem. 100 (1996) 17801.
[46] R. West, J.J. Buffy, M. Haaf, T. Muller, B. Gehrhus, M.F. Lappert, Y. Apeloige, J. Am. Chem. Soc. 120 (1998) 1639.
[47] Y. Apeloig, R. Pauncz, M. Karni, R. West, W. Steiner, D. Chapman, Organometallics 22 (2003) 3250.
[48] R.S. Grev, H.F. Schaefer III, P.P. Gaspar, J. Am. Chem. Soc. 113 (1991) 5638.
[49] R.S. Grev, H.F. Schaefer III, J. Am. Chem. Soc. 108 (1986) 5804.
[50] C.G. Swain, S.H. Unger, N.R. Rosenquist, S.M. Swain, J. Am. Chem. Soc. 105 (1983) 492.